

Sliding Mode Control-Based Standalone Wind Energy System



R. M. Meenakshi and K. Selvi

1 Introduction

The conflict in growing need of electricity and age old way of long distribution lines paves way for an economic alternative, namely the microgrids. A microgrid is a low-voltage network with small-scale power generation units, energy storage devices and loads [1]. The present trend in microgrid is the power generation from renewable energy sources. Microgrid with renewable resources can help to eradicate the environmental concerns due to fossil fuels. As the nature of renewable sources and the modern day load are predominantly DC, the need for a common DC interface arises. The integration of present AC utility grid and the DC sub-grids evolves a complex network of hybrid AC/DC microgrids [2]. The power conversion between the DC and AC interface is performed with the interlinking converters. These power converters act as a brain of the microgrids by controlling the voltage and current levels. The efficiency of power transfer in microgrid relies on the proper control strategy to control the operation of switching converters. Since the last decade, many researchers have suggested different control strategies for stable operation of microgrid [3, 4]. The conventional cascaded linear control and the droop control techniques are widely discussed for various configuration and operating scenarios of microgrid [5–8]. These techniques suffer from slow response, complex tuning of control parameters and inefficiency in accommodating multiple constraints. One of the main issues in employing renewable energy sources for generation is the intermittent nature of power output.

R. M. Meenakshi (✉) · K. Selvi
Department of Electrical and Electronics Engineering, Thiagarajar College of Engineering,
Madurai, TN 625015, India
e-mail: meenakshirm1@student.tce.edu

K. Selvi
e-mail: kseee@tce.edu

The linear controllers fail to dynamically adapt for the varying operating condition and the environment. Following the linear controllers, many works report the performance of the fuzzy [9] and neural network [10] controllers. These works majorly represents microgrid with single sources. Also, they emphasize on providing a clear knowledge about different operating scenarios to the controller. This makes the controller inefficient during uncertainties. As the renewable resources do not provide continuous power output, it is necessary to take care of reliability in power supply. The energy storage systems and other reliable energy sources can ensure the continuity of power supply in microgrid. The controller must promptly respond under all operating conditions, handling multiple sources and loads. In view of these necessities, the research studies have shifted the focus on nonlinear controllers. Certain nonlinear controllers, namely backstepping controller [11], sliding mode controllers, etc., have been widely discussed for both grid interfaced and standalone microgrids.

Among these controllers, the sliding mode control (SMC) strategy shows a fast dynamic response and ensures system stability. The SMC is featured by its robustness against any disturbances. In a previous research work [12], this controller is employed for power extraction in DC sources by tracking the parameters at device level of renewables. The control of power flow between the system and the battery is less reported. Though the SMC proves better when two wind energy conversion systems interact with the grid [13], both the machines will fail to supply the loads under less windy conditions. This can increase the burden on the grid. Also these works partly still rely on PI controllers for error tracking of parameters. This can deteriorate the performance of SMC. This controller is further reported for solar photovoltaic systems, and the performance is analyzed for standalone mode [14]. The power balance between the DG source and energy storage system with the help of SMC can prove to be a better solution in handling the uncertainties of the environment and other operating disturbances.

This paper aims to analyze the performance of SMC in a Wind PMSG-battery based standalone microgrid. The aim of our work is to employ the sliding mode control approach to obtain: (1) optimal power output from wind energy according to wind speed variations, (2) bidirectional power flow control between the battery storage system and the microgrid and (3) ensure stable operation of the microgrid under all operating conditions. Further sections present the description of components in microgrid, the modeling of each component with the corresponding power electronic converters, the application of sliding mode strategy and the discussion on results under a few operating scenarios.

2 Description of Proposed Wind-Battery Microgrid

In this paper, a standalone microgrid based on PMSG-battery system is presented, as shown in Fig. 1. The proposed system consists of PMSG-driven wind energy system, a switched mode rectifier, battery storage system with a bidirectional DC-DC converter, DC link capacitor, voltage source inverter, LC filters and AC-DC loads.

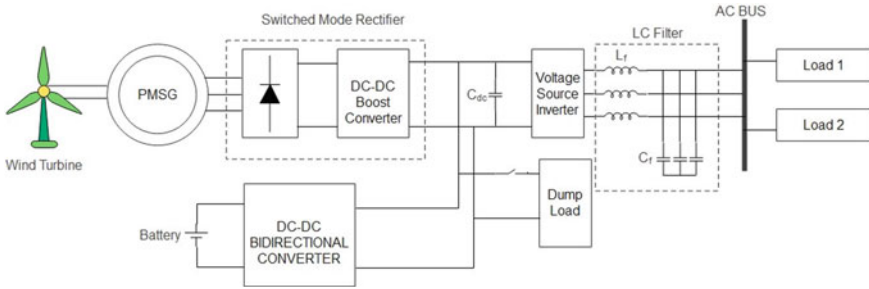


Fig. 1 Proposed standalone microgrid

A SMC-based controller is proposed to control the power electronics converters in the proposed system. Appendix I gives the detailed specifications of each component.

3 Modeling of Wind Energy Conversion Systems

A wind energy system as in Fig. 2 is modeled with a wind turbine driving the PMSG machine directly without any gear box. The output of the PMSG machine is controlled by employing a switched mode rectifier built with diode rectifier and DC-DC boost converter. A wind turbine system converts kinetic energy into mechanical energy to drive the electrical machine to generate power. The mechanical power extracted by the wind turbine is given by,

$$P_m = 0.5 * \rho * C_p(\lambda, \beta) * A * v_w^3 \tag{1}$$

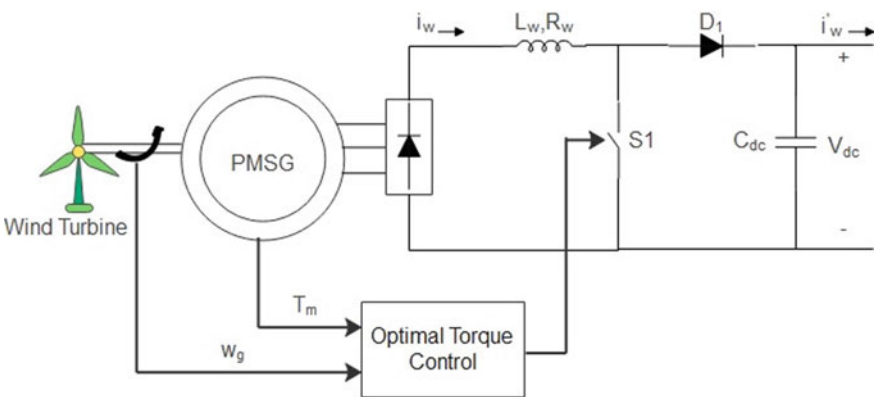


Fig. 2 Wind energy system

where C_p is the coefficient of performance, λ is the tip speed ratio (TSR), β is the pitch angle, A is the area of turbine blade (m^2), ρ is the air density (kg/m^3), and v_w is the wind velocity (m/s^2).

To extract maximum power from the wind turbine, the optimum tip speed ratio required is,

$$\lambda_{opt} = \frac{\omega_w * r}{v_w} \tag{2}$$

where ω_w is the angular speed of the rotor (rad/s) and r is the turbine radius (m).

By substituting for wind speed v_w in (1), the optimum mechanical power from the turbine is obtained as,

$$P_m = 0.5\rho\pi r^5 \frac{\omega_m^3}{\lambda_{opt}^3} C_{pmax} \tag{3}$$

where C_{pmax} is the maximum power coefficient to achieve MPPT. Equation (3) can be written as,

$$P_{m-op} = K_{p-op}\omega_m^3 \tag{4}$$

where

$$K_{p-op} = 0.5\rho\pi r^5 \frac{C_{pmax}}{\lambda_{op}^3}$$

As per the torque power relationship, $P_{m-op} = \omega_m T_{m-op}$, and from Eq. (4), the expression for optimum torque can be expressed as

$$T_{m-op} = K_{p-op}\omega_m^2 \tag{5}$$

To extract the maximum power, by using optimum torque control (OTC) technique, a reference torque related to the reference current I_{wref} is determined by the following equation:

$$I_{wref} = \frac{T_{m-op} * \omega_m}{V_w} \tag{6}$$

where V_w is the output DC voltage measured from the DC side of diode rectifier. The voltage and current equations for the DC-DC converter can be derived as follows:

$$\begin{bmatrix} \frac{dI_w}{dt} \\ \frac{dV_{dc}}{dt} \end{bmatrix} = \begin{bmatrix} -\frac{R_w}{L_w} & -(1-d_1)\frac{1}{L_w} \\ (1-d_1)\frac{1}{C_{dc}} & 0 \end{bmatrix} \begin{bmatrix} I_w \\ V_{dc} \end{bmatrix} + \begin{bmatrix} \frac{1}{L_w} \\ 0 \end{bmatrix} V_w + \begin{bmatrix} 0 \\ -\frac{1}{C_{dc}} \end{bmatrix} I'_w \tag{7}$$

where I_w , V_{dc} and d_1 are the wind current, DC link voltage and the pulse signal for boost converter switch S_1 , respectively.

4 Modeling of Battery Storage System

A lead acid battery is designed to balance the power in the microgrid system with proper discharging and charging using a bidirectional buck boost converter as shown in Fig. 3. The battery is coupled to the PMSG system at the DC link through the converter. The voltage and current equation of the converter can be written as:

$$\begin{bmatrix} \frac{dI_{\text{bat}}}{dt} \\ \frac{dV_{\text{dc}}}{dt} \end{bmatrix} = \begin{bmatrix} -\frac{R_{\text{bat}}}{L_{\text{bat}}} & -d_{23} \frac{1}{L_{\text{bat}}} \\ d_{23} \frac{1}{C_{\text{dc}}} & 0 \end{bmatrix} \begin{bmatrix} I_{\text{bat}} \\ V_{\text{dc}} \end{bmatrix} + \begin{bmatrix} \frac{1}{L_{\text{bat}}} \\ 0 \end{bmatrix} V_{\text{bat}} + \begin{bmatrix} 0 \\ -\frac{1}{C_{\text{dc}}} \end{bmatrix} I'_{\text{bat}} \quad (8)$$

where I_{bat} , V_{dc} and d_{23} are the battery current, DC link voltage and the control signal for the switches S_2 and S_3 of the bidirectional converter.

5 Sliding Mode Control of Wind and Battery Converters

Figure 4 shows the schematic implementation of sliding mode control. The main purpose of the controller discussed in this paper is:

1. DC bus voltage regulation at point of common coupling of wind and energy storage system.
2. Reliable supply to the AC loads in standalone mode.

For proper control operation, the error tracking trajectories are given as:

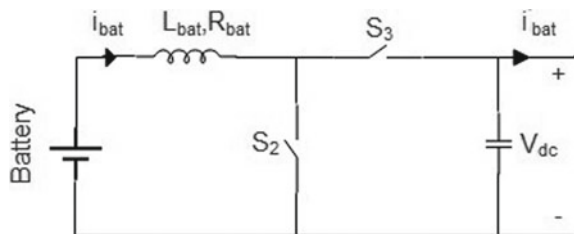
$$\begin{Bmatrix} e_1 \\ e_2 \end{Bmatrix} = \begin{Bmatrix} x_1 - x_1^* \\ x_2 - x_2^* \end{Bmatrix} \quad (9)$$

where x_1^* and x_2^* are the wind and battery reference currents. The basic necessity of a sliding mode controller is to define a sliding surface for each control parameter. The sliding surfaces are given by the error surfaces as:

$$S_1 = e_1 \quad (10)$$

$$S_2 = e_2 \quad (11)$$

Fig. 3 Bidirectional battery converter



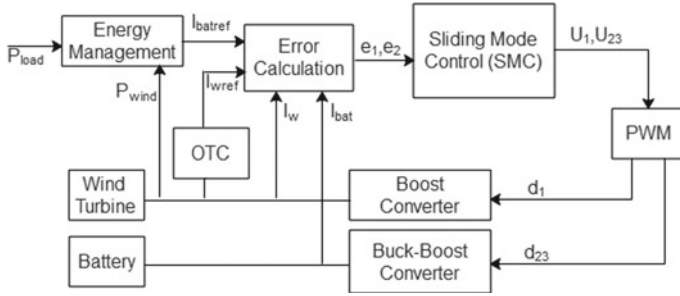


Fig. 4 Proposed controller structure

Next, the derivative of the sliding surface is given as

$$\dot{S}_1 = \dot{e}_1 \tag{12}$$

$$\dot{S}_2 = \dot{e}_2 \tag{13}$$

Substituting for \dot{e}_1 in (12) gives:

$$\dot{S}_1 = \frac{V_w}{L_w} - \frac{R_w}{L_w}x_1 - (1 - d_1)\frac{x_3}{L_w} - x_1^* \tag{14}$$

To achieve stable operation, the derivative of surface must be selected as:

$$\dot{S}_k = -\rho_k \text{sgn}(S_k) \tag{15}$$

where $\rho_k > 0$ and $k = 1, 2$. The sgn represents the signum function and can be written as:

$$\text{sgn}(x) = \begin{cases} \frac{x}{|x|} & x \neq 0 \\ 0 & x=0 \end{cases} \tag{16}$$

By applying (15) in (14), the control law d_1 can be obtained as

$$d_1 = \frac{L_w}{x_3}[-\rho_1 \text{sgn}(S_1) - \frac{V_w}{L_w} + \frac{R_w}{L_w}x_1] + \frac{L_w}{x_3}[x_1^*] + 1 \tag{17}$$

The d_1 is the duty cycle signal applied to the boost converter of wind energy system connected at the common DC bus. It is bounded by $0 < d_1 < 1$. For a battery storage system, the derivative of sliding surface and the control law can be obtained as:

$$\dot{S}_2 = \frac{V_{bat}}{L_{bat}} - \frac{R_{bat}}{L_{bat}}x_2 - x_3^* \tag{18}$$

$$d_{23} = \frac{L_{bat}}{x_3} [\rho_2 \text{sgn}(S_2) + \frac{V_{bat}}{L_{bat}} - \frac{R_{bat}}{L_{bat}} x_2] + \frac{L_{bat}}{x_3} - x_2^* \tag{19}$$

where d_{23} is the duty cycle signal for the bidirectional converter between the battery and DC bus system. It is bounded between 0 and 1.

The control signals for the voltage source inverter are provided by the conventional DC control according to the implementation in [15].

6 Results and Discussion

The proposed control strategy was implemented in the MATLAB/SIMULINK platform, with detailed design of each system components in standalone microgrid. The wind speed and load disturbances are applied similar to the practical scenarios, in order to analyze the robustness of the sliding mode controller. Such variations are employed to show how effectively the proposed controller regulates the DC bus voltage. The controller performance is assessed under two conditions, namely (a) variable load and (b) fluctuating wind conditions. Combining these two scenarios, the stability of DC link, power balance by the energy storage system and optimal power extracted from wind were investigated. Figure 5 shows the variations in wind profile, and step changes in load are presented. The AC linear loads of 3, 2 and 2 kW are each stepped in at $t = 0, 7$ and 14s. The wind speed varies continuously withing the range of 11–13m/s.

Initially, the battery SOC is 65%. The constant load prevailing in the microgrid is 3 kW. The wind power generation is around 6 kW as per the PMSG machine rating. The excess power is employed to charge the battery. Figures 6a–b show the wind power generation and increase in battery SOC. At $t = 7$ s, a load disturbance of 2kW is introduced. The battery still charges at a slower rate, while wind energy supplied to the change in load. Followed by this, another load of 2 kW is again introduced at $t = 14$ s, where the load demand becomes higher than the generation. At this point, the battery starts to discharge and supports to maintain the power balance in the microgrid.

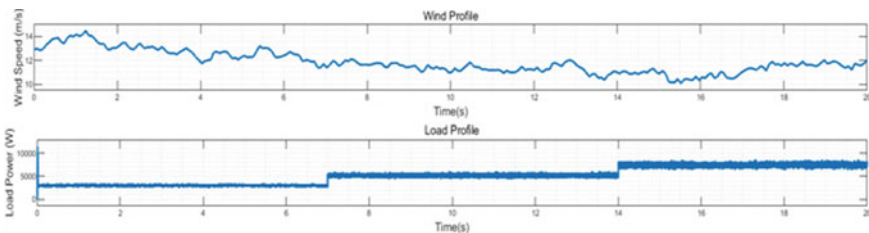


Fig. 5 Wind and load profile

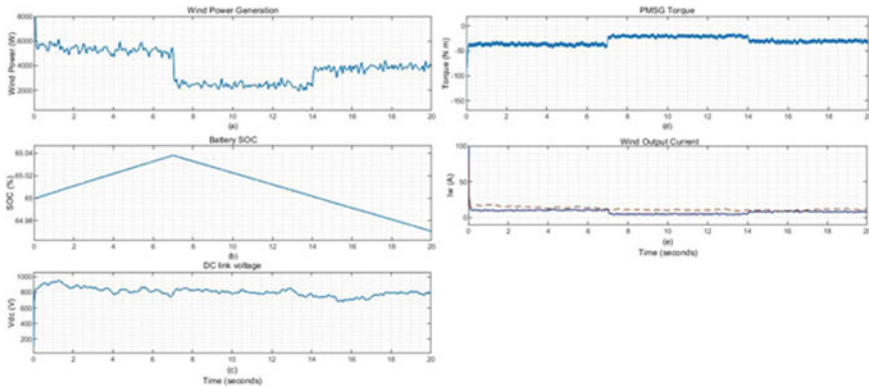


Fig. 6 a Wind power. b Battery SOC. c DC link voltage. d PMSG torque. e Wind output current

Table 1 PI and SMC controller specifications

Specifications	SMC controller	PI controller
Overshoot	18.0457%	24.1356%
Settling time (s)	19.9391	19.9360
Peak time (s)	1.2739	1.2732

During such continuous wind variations and step changes in load, the DC link voltage as shown in Fig. 6c is maintained constant. The stabilization of DC link voltage achieved by the sliding mode control strategy is compared with the conventional PI controller. From this comparison, it is seen that the overshoot due to proposed SMC controller is lower compared to the conventional controller. The table shows the time-domain specification comparison of the two controllers (Table 1).

Figure 6d confirms the optimal torque control showing constant torque for the PMSG machine, which is achieved by tracking the diode rectifier output current (Fig. 6e) as per Eq. 6.

Under similar conditions of wind speed and load changes, the case of battery SOC of 95% is examined. In this scenario, during excess power generation, a dump load is introduced to balance the DC link voltage. Figure 7a shows that battery only discharges when there is a demand in power at $t = 14$ s with a 2 kW load disturbance. Until then, the battery remains ideal, diverting the power to the dump load. Figure 7b shows that the DC link voltage remains constant as balanced by the dump load. Figure 7c shows the dump load power support during excess generation duration of 0–14s. Figure 8 shows that the AC side load voltage is maintained with the load current variations according to the load profile.

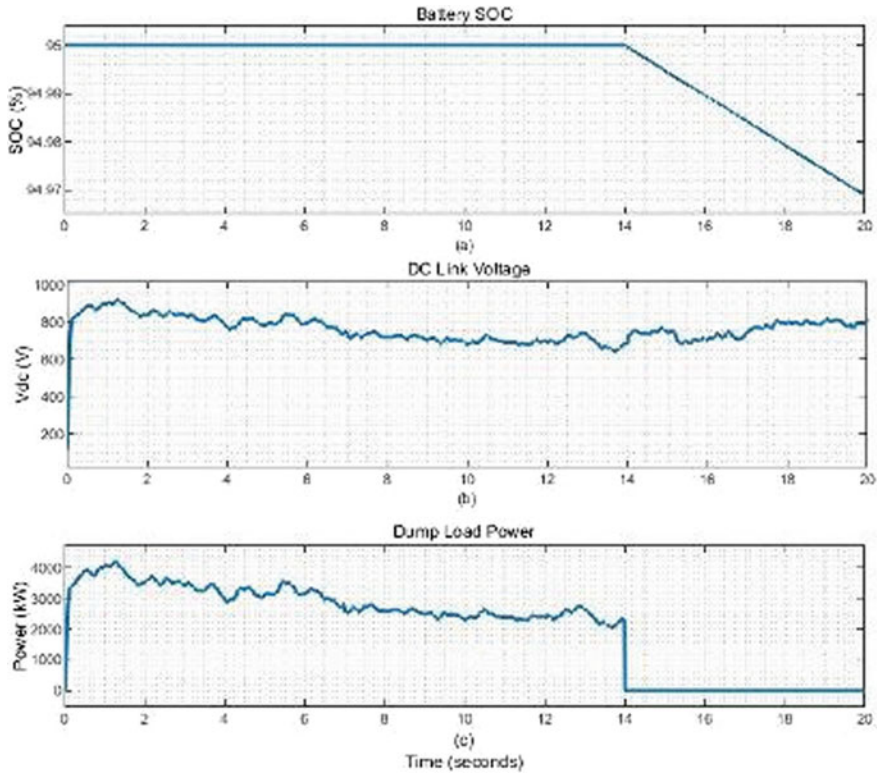


Fig. 7 a Battery SOC. b DC link voltage. c Dump load power

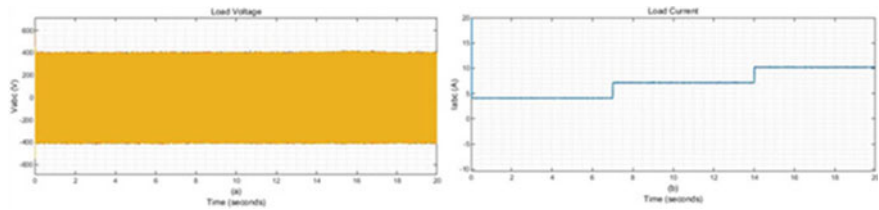


Fig. 8 a Load voltage and b Load current

7 Conclusion

This paper presents the design and analysis of sliding mode controller for maintaining DC link voltage and power balance in the standalone hybrid AC/DC microgrid. The performance of the SMC is evaluated under certain scenarios in the SIMULINK environment. It is seen that the dynamics in wind profile and load changes are better addressed by the sliding mode controller in comparison to the PI controller. Also,

the battery storage system effectively participates under excess and deficit power demands. The parameters of SMC can be tuned easier in comparison to the PI controllers. It is seen that though the SMC provides a better adaptation to disturbances, still further improvements are much necessary to tightly control the DC link voltage. To overcome such limitations, one or more reliable generation source could be further introduced for proper power balance. Also, the controller could be better designed to handle the higher order dynamics. Further, the control approach could be extended to the interaction of microgrid with utility grid and transition between islanded and grid-connected modes.

Acknowledgements This research work was supported by the Research Excellence strand of Savitha Project-Thiagarajar Research Fellowship under Ref: TCE/Dean-RD/TRF (2020–2023).

Appendix

Design Specifications

Wind turbine model

Air density	1.225 kg/m ³
Rated wind speed	12 m/s
Rotor diameter	1.16 m
λ_{opt}	7.5
C_p	0.43
<i>PMSG</i>	
Stator phase resistance	0.425 Ω
Armature inductance	8.5 mH
Flux linkage	0.433 Wb
Pole pairs	5
Rated speed	153 rad/s
<i>Lead acid battery</i>	
Voltage	300 V
Rated capacity	35 AH
Maximum charge current	7.2 A
Maximum discharge current	10 A
<i>AC/DC microgrid parameters</i>	
DC grid voltage	800 V
AC grid voltage	400 V
Frequency	50 Hz
DC bus capacitor	1500 μ F
AC bus LC filter	$L_f = 1$ mH, $C_f = 100$ μ F
AC loads	Load 1 = 3 KW , Load 2= 2kW, 2kW

References

1. Mahmoud MS, Azher Hussain S, Abido MA (2014) Modeling and control of microgrid: an overview. *J Franklin Inst* 351(5):2822–2859. <https://doi.org/10.1016/j.jfranklin.2014.01.016>
2. Gupta A, Doolla S, Chatterjee K (2018) Hybrid AC-DC microgrid: systematic evaluation of control strategies. *IEEE Trans Smart Grid* 9(4):3830–3843. <https://doi.org/10.1109/TSG.2017.2727344>
3. Nikam V, Kalkhambkar V (2021) A review on control strategies for microgrids with distributed energy resources, energy storage systems, and electric vehicles. *Int Trans Electr Energy Syst* 31(1):1–26. <https://doi.org/10.1002/2050-7038.12607>
4. Olivares DE, Mehrizi Sani A, Etemadi AH, Cañizares CA, Iravani R, Kazerani M, Hajimiragha AH, Gomis Bellmunt O, Saeedifard M, Palma-Behnke R, Jiménez-Estévez GA, Hatziargyriou ND (2014) Trends in microgrid control. *IEEE Trans Smart Grid* 5(4):1905–1919. <https://doi.org/10.1109/TSG.2013.2295514>
5. Fazeli M, Holland P (2017) Universal and seamless control of distributed resources–energy storage for all operational scenarios of microgrids. *IEEE Trans Energy Convers* 32(3):963–973. <https://doi.org/10.1109/TEC.2017.2689505>
6. Eghtedarpour N, Farjah E (2014) Power control and management in a Hybrid AC/DC microgrid. *IEEE Trans Smart Grid* 5(3):1494–1505. <https://doi.org/10.1109/TSG.2013.2294275>
7. De Matos JG, Silva E, Ribeiro LAS (2015) Power control in AC isolated microgrids with renewable energy sources and energy storage systems. *IEEE Trans Indus Electron* 62(6):3490–3498. <https://doi.org/10.1109/TIE.2014.2367463>
8. Tayab UB, Bin Roslan MA, Hwai LJ, Kashif M (2017) A review of droop control techniques for microgrid. *Renew Sustain Energy Rev* 76:717–727. <https://doi.org/10.1016/j.rser.2017.03.028>
9. Muyeen SM, Al-Durra A (2013) Modeling and control strategies of fuzzy logic controlled inverter system for grid interconnected variable speed wind generator. *IEEE Syst J* 7(4):817–824. <https://doi.org/10.1109/JSYST.2013.2239893>
10. Singh P, Lather JS (2020) Artificial neural network-based dynamic power management of a DC microgrid: a hardware-in-loop real-time verification. *Int J Ambient Energy* 1–19. <https://doi.org/10.1080/01430750.2020.1720811>
11. Boujmil MH, Badis A, Nejib Mansouri M (2018) Nonlinear robust backstepping control for three-phase grid-connected PV systems. *Math Probl Eng*. <https://doi.org/10.1155/2018/3824628>
12. Baghaee HR, Mirsalim M, Gharehpetian GB, Talebi HA (2017) A decentralized power management and sliding mode control strategy for hybrid AC/DC microgrids including renewable energy resources. *IEEE Trans Indus Inform* 3203(c):1–1. <https://doi.org/10.1109/tii.2017.2677943>
13. Errami Y, Ouassaid M, Maaroufi M (2015) A performance comparison of a nonlinear and a linear control for grid connected PMSG wind energy conversion system. *Int J Electr Power Energy Syst* 68:180–194. <https://doi.org/10.1016/j.ijepes.2014.12.027>
14. Rezkallah M, Hamadi A, Chandra A, Singh B (2015) Real-time HIL implementation of sliding mode control for standalone system based on PV array without using dumpload. *IEEE Trans Sustain Energy* 6(4):1389–1398. <https://doi.org/10.1109/TSSTE.2015.2436333>
15. Bhende CN, Mishra S, Malla SG (2011) Permanent magnet synchronous generator-based standalone wind energy supply. *System* 2(4):361–373